Journal of Orthopaedic Translation 37 (2022) 46–60

Contents lists available at ScienceDirect

Journal of Orthopaedic Translation

journal homepage: www.journals.elsevier.com/journal-of-orthopaedic-translation

Fecal microbiota transplantation ameliorates bone loss in mice with ovariectomy-induced osteoporosis via modulating gut microbiota and metabolic function

Yuan-Wei Zhang [a,b,c,d,e], Mu-Min Cao [a,b,c,d,e], Ying-Juan Li [b,f], Pan-Pan Lu [a,b,c,d,e], Guang-Chun Dai [a,b,c,d,e], Ming Zhang [a,b,c,d,e], Hao Wang [a,b,c,d,e], Yun-Feng Rui [a,b,c,d,e,*]

[a] Department of Orthopaedics, Zhongda Hospital, School of Medicine, Southeast University, Nanjing, Jiangsu, PR China
[b] Multidisciplinary Team (MDT) for Geriatric Hip Fracture Management, Zhongda Hospital, School of Medicine, Southeast University, Nanjing Jiangsu, PR China
[c] School of Medicine, Southeast University, Nanjing, Jiangsu, PR China
[d] Orthopaedic Trauma Institute (OTI), Southeast University, Nanjing, Jiangsu, PR China
[e] Trauma Center, Zhongda Hospital, School of Medicine, Southeast University, Nanjing, Jiangsu, PR China
[f] Department of Geriatrics, Zhongda Hospital, School of Medicine, Southeast University, Nanjing, Jiangsu, PR China

ARTICLE INFO

Keywords:
Fecal microbiota transplantation
Ovariectomy-induced osteoporosis
Bone loss
Gut microbiota
Short chain fatty acids

ABSTRACT

Background: Osteoporosis (OP) is a systemic metabolic bone disease characterized by decreased bone mass and destruction of bone microstructure, which tends to result in enhanced bone fragility and related fractures. The postmenopausal osteoporosis (PMOP) has a relatively high proportion, and numerous studies reveal that estrogen-deficiency is related to the imbalance of gut microbiota (GM), impaired intestinal mucosal barrier function and enhanced inflammatory reactivity. However, the underlying mechanisms remain unclear and the existing interventions are also scarce.

Methods: In this study, we established a mouse model induced by ovariectomy (OVX) and conducted fecal microbiota transplantation (FMT) by gavage every day for 8 weeks. Subsequently, the bone mass and micro-architecture of mice were evaluated by the micro computed tomography (Micro-CT). The intestinal permeability, pro-osteoclastogenic cytokines expression, osteogenic and osteoclastic activities were detected by the immunohistological analysis, histological examination, enzyme-linked immunosorbent assay (ELISA) and western blot analysis accordingly. Additionally, the composition and abundance of GM were assessed by 16S rRNA sequencing and the fecal short chain fatty acids (SCFAs) level was measured by metabolomics.

Results: Our results demonstrated that FMT inhibited the excessive osteoclastogenesis and prevented the OVX-induced bone loss. Specifically, compared with the OVX group, FMT enhanced the expressions of tight junction proteins (zonula occludens protein 1 (ZO-1) and Occludin) and suppressed the release of pro-osteoclastogenic cytokines (tumor necrosis factor-α (TNF-α) and interleukin-1β (IL-1β)). Furthermore, FMT also optimized the composition and abundance of GM, and increased the fecal SCFAs level (mainly acetic acid and propionic acid).

Conclusions: Collectively, based on GM-bone axis, FMT prevented the OVX-induced bone loss by correcting the imbalance of GM, improving the SCFAs level, optimizing the intestinal permeability and suppressing the release of pro-osteoclastogenic cytokines, which may be an alternative option to serve as a promising candidate for the prevention and treatment of PMOP in the future.

Abbreviations: OP, osteoporosis; PMOP, postmenopausal osteoporosis; RANKL, receptor activator for nuclear factor-κB ligand; IL-1β, interleukin-1β; TNF-α, tumor necrosis factor-α; GM, gut microbiota; FMT, fecal microbiota transplantation; OVX, ovariectomy; BMD, bone mineral density; TRAP, tartrate-resistant acid phosphatase; OPN, osteopontin; OPG, osteoprotegerin; RUNX2, recombinant runt related transcription factor 2; ZO-1, zonula occludens protein 1; SCFAs, short chain fatty acids; TRACP5B, tartrate-resistant acid phosphatase 5B; PCoA, principal coordinates analysis; OTU, operational taxonomic unit; NMDS, non-metric multi-dimensional scaling; QIIME, quantitative insights into microbial ecology; KEGG, kyoto encyclopedia of genes and genomes; OPLS-DA, orthogonal partial least squares discriminant analysis.

* Corresponding author. Department of Orthopaedics, Zhongda Hospital, School of Medicine, Southeast University, No. 87 Ding Jia Qiao, Nanjing, Jiangsu, 210009, PR China.
E-mail address: ruiyunfeng@126.com (Y.-F. Rui).

https://doi.org/10.1016/j.jot.2022.08.003
Received 6 May 2022; Received in revised form 29 July 2022; Accepted 8 August 2022

2214-031X/© 2022 The Authors. Published by Elsevier B.V. on behalf of Chinese Speaking Orthopaedic Society. This is an open access article under the CC BY-NC-ND license (http://creativecommons.org/licenses/by-nc-nd/4.0/).

The translational potential of this article: This study indicates the ingenious involvement of GM-bone axis in PMOP and the role of FMT in reshaping the status of GM and ameliorating the bone loss in OVX-induced mice. FMT might serve as a promising candidate for the prevention and treatment of PMOP in the future.

1. Introduction

Osteoporosis (OP) is a kind of systemic bone disease characterized by decreasing bone mass and destruction of bone microstructure, which easily leads to the enhanced bone fragility and associated fractures [1,2]. Therein, the postmenopausal osteoporosis (PMOP) accounts for more than 80%, and usually accompanied by a high incidence of brittle fractures, as well as the high rates of disability and mortality, which severely threatens the health of the middle-aged and elderly women and brings an incrementally heavy burden to the social medical service systems [3]. Currently, the prevention and treatment of PMOP mainly depends on the lifestyle adjustments and various types of drug interventions [4,5]. On the basis of this, with the continuous advancement of aging process around the world, it is still necessary to explore and verify more effective prevention and treatment strategies for PMOP.

Up to now, the initiation factor of PMOP is considered to be the lack of estrogen caused by postmenopausal ovarian failure, and the excessive formation and absorption of osteoclasts are regarded as the vital pathological changes [6,7]. With regard to this, previous research evidence indicates that receptor activator for nuclear factor-κB ligand (RANKL) is an essential factor involved in the regulation of osteoclasts, and the main driving factors of increased osteoclastogenesis are the enhanced production of RANKL and pro-osteoclastogenic cytokines, which includes interleukin-1β (IL-1β), IL-6, tumor necrosis factor-α (TNF-α) [8,9]. On this basis, RANKL/RANK/OPG pathway plays a critical role in the regulation of bone resorption and bone formation [3,10–13]. Moreover, recent emerging evidence have also revealed that the estrogen-deficiency is able to induce the imbalance of gut microbiota (GM), impaired intestinal mucosal barrier function, and enhanced inflammatory system reactivity [14–16]. During this process, the metabolites of intestinal pathogenic bacteria can enter the body through the damaged intestinal mucosal barrier, further trigger the immune response mediated by CD4+T cells and generate the pro-osteoclastogenic cytokines, and ultimately promote the activation of osteoclasts, which further highlights the existence and significance of GM-bone axis [17]. Moreover, in our previous critical reviews, based on the concept of "brain-gut-bone" axis, we have also summarized the modulatory effects and implication of GM to OP [18], as well as the regulative effects and repercussion of probiotics and prebiotics on OP [19]. Hence, in view of the close relationship between GM and bone metabolism, it is acknowledged that GM may can be regarded as a potential target for the prevention and treatment of OP to a certain extent.

To date, the treatment strategies of intervening GM mainly include antibiotic use, diet adjustments, probiotic supplementation and fecal microbiota transplantation (FMT) [20,21]. Therein, FMT, as an emerging kind of "organ transplantation", has gradually attracted more and more attention from the scholars. Briefly, FMT treatment is a novel method to transplant the flora in donor feces to recipient by the means of gavage or oral administration, which is committed to altering the composition and abundance of the GM in recipient's intestine [22]. In this process, FMT treatment remodels the intestinal microecology and also improves the inflammatory, immune and metabolic status of the recipient, providing an emerging therapeutic concept and approach for several intestinal and non-intestinal diseases [23,24]. Up to now, FMT treatment has been verified to be effective in various intestinal diseases, such as ulcerative colitis, Crohn's disease and colon cancer. Meanwhile, it also been widely explored and applied in several metabolic and immune diseases, such as obesity, diabetes mellitus, arthritis, and so on [25–31]. However, to the best of our knowledge, there is still no evidence of FMT treatment on the PMOP currently, and none is known about its feasibility and effectiveness. Hence, we conducted this current study and hypothesized that FMT treatment from healthy mice into the mice with ovariectomy (OVX)-induced OP may remodel the GM and ameliorate the bone loss to a certain extent.

2. Materials and methods

2.1. Preparation of animals and PMOP models establishment

Overall animal experimental designs and schemes were approved by Institutional Animal Care and Use Committee (IACUC) in the School of Medicine, Southeast University (No. 20210510012). Eight-week-old female C57BL/6 mice were purchased from Payi Organism Co., Lrd. (Nanjing, Jiangsu, China), housed under the specific pathogen-free (SPF) conditions, and maintained under standard laboratory conditions (temperature, 25 ± 2 °C; humidity, 50 ± 5%), with a 12h:12h light/dark cycle. The food and water were available ad libitum. The detailed operation procedures of OVX were conducted as described in previous report [32]. In brief, after being anesthetized with 1% sodium pentobarbital solution (40 mg/kg), the mice were placed in the prone position and a single longitudinal incision at midline dorsal skin (approximately 1 cm) was made. Subsequently, the muscle fibers were separated by the tip of tissue scissors, and bilateral ovaries were further located, identified and removed in turns. Subsequently, the cotton swabs were used to stop bleeding, and the incision was further closed layer by layer with absorbable sutures.

2.2. Animals experimental design

The schematic representation of the experiments was exhibited in Fig. 1. As shown in Fig. 1A, after 1-week environment acclimatization, the mice were randomly assigned to four groups, including Sham group, OVX group, OVX + normal saline (NS) group, and OVX + FMT group, with a total of 20 mice (5 mice in each group). Simple size was determined based on "4R" principles advocated by animal protection and animal welfare organizations and prompted by previous reports [15,33]. For Sham group, except reserving ovaries, the mice underwent the same procedures as above. The mice in OVX group underwent the ovariectomy and were treated as the vehicle. On the basis of OVX, the mice in the OVX + NS group and OVX + FMT group received the gavage of NS and donor FMT materials once a day for the consecutive 8 weeks, starting at the 1 week after OVX/Sham operation and until 1 day before sacrifice. The body weight of mice in each group was also monitored every two weeks. After finishing the last gavage at 1 day before sacrifice, the mice were deprived of food for 12h, and fecal samples were then collected and stored at −80 °C. At the end of whole experiments, the mice were weighed and sacrificed, and the femurs, serum and colonic tissues (1 cm next to the cecocolic junction) of mice [34] in all groups were collected for further corresponding analysis (Fig. 1B).

2.3. Preparation of donor fecal transplant materials and FMT treatment

The overall preparation of donor fecal transplant materials was referred to previous experimental researches with the similar assay [21]. In brief, 20 healthy C57BL/6 mice raised in the same environment, with same weeks old and sex, were considered as the fecal donors. In the experimental cycle, at 9:00 a.m. every day, the anal stimulation method was used to induce the healthy mice to excrete fresh feces (20–30 pellets), and the NS was further added, mixed and dissolved evenly (1 pellet/1 ml NS, vortexed for about 0.5 min until there was no visible fecal

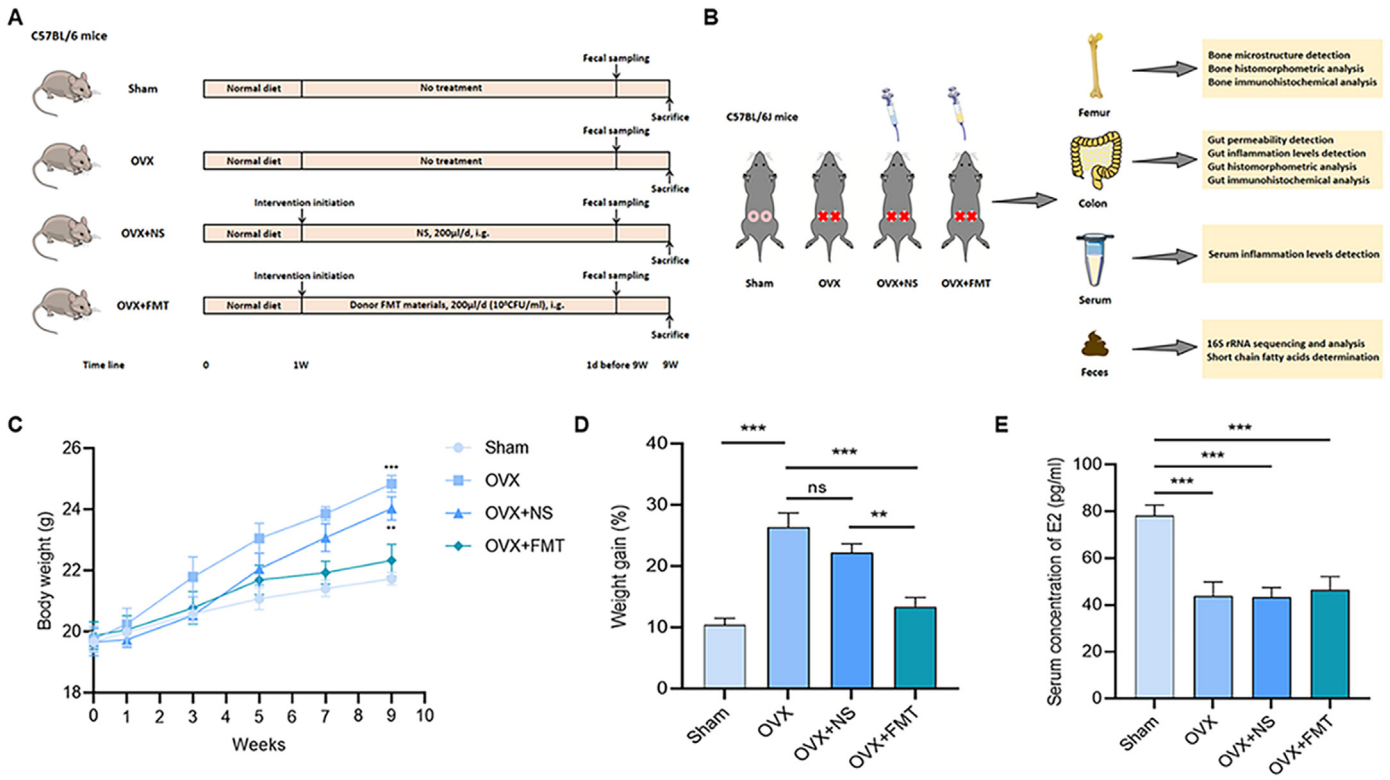

Figure 1. The schematic representation of experiments, effects of the FMT treatment on the body weight and serum E2 concentrations in mice with OVX-induced OP. (A–B) The schematic representation of the overall experiments (C) The body weight of mice in all groups, and the different letters represented significant differences compared with OVX + FMT group; (D) Weight gain of mice in all groups (E) Serum concentration of E2. Data were expressed as mean ± SD ($n = 5$). One-way ANOVA procedure followed by the Tukey test and Pearson's correlation were used to assess statistical significance. Different letters represented significant differences between different groups, $^{*}P < 0.05$, $^{**}P < 0.01$, and $^{***}P < 0.001$ compared with the corresponding group.

particles in solution). Next, the obtained samples were then centrifuged at 2000 rpm and 4 °C for 10 min, the fecal residue was discarded, and the supernatant was taken. The supernatant was then centrifuged again at 8000 rpm and 4 °C for 5 min to obtain the total bacteria, then mixed with NS and prepared for further implementation of FMT treatment [35]. Moreover, for the mice in OVX + FMT group, 200 μl of bacterial suspension (10^8 CFU/ml) [21] was transplanted to the recipient mice by gavage once a day for consecutive 8 weeks. For the mice in OVX + NS group, the recipient mice received 200 μl of NS by gavage once a day for consecutive 8 weeks.

2.4. Micro-computed tomography (CT) scanning

The micro-CT scanning device (SkyScan 1176, Bruker, Karlsruhe, Germany), with the parameters (voltage: 70 kV, current: 200 μA, resolution: 9 μm), was used to assess the femoral structure of mice. During the process of scanning, a 0.5 mm thick aluminum filter was applied to reduce the beam hardening. Images were then reconstructed using NRecon software (Bruker, Karlsruhe, Germany) and conducted three-dimensional (3D) model visualization in CTVol software (Bruker, Karlsruhe, Germany). Furthermore, the quantitative morphometric analysis was conducted on the region of interest (ROI) of 50 cross-sectional planes (0.5 mm) below the femoral growth plate, so as to further analyze 200 cross-sectional planes with height (2 mm) for trabecular bone. Then, the structural parameters of the region of femur were further analyzed using program CTAn (Bruker, Karlsruhe, Germany), which included bone mineral density (BMD, g/cc), bone surface area/total volume (BS/TV, 1/mm), bone volume/total volume (BV/TV, %), trabecular number (Tb.N, 1/mm), trabecular space (Tb.Sp, mm), and trabecular thickness (Tb.Th, mm).

2.5. Histological and histomorphometric analysis

After the detection of micro-CT scanning, femurs and colonic tissues of mice in all groups were fixed in the 4% paraformaldehyde (Servicebio, Wuhan, Hubei, China) for 24 h, and then the 12.5% ethylene diamine tetraacetic acid (EDTA, Servicebio, Wuhan, Hubei, China) was applied for femoral decalcification for another 3–4 weeks. Moreover, the tissues were embedded in the paraffin, and the histological sections with 5 μm thick were made. Then, the sections of femurs and colonic tissues underwent the hematoxylin and eosin (H&E) staining, and the tartrate-resistant acid phosphatase (TRAP) staining was further applied to assess the osteoclastogenesis of femurs. Furthermore, the number of osteoclasts were quantified using the Image J software (National Institutes of Health, Bethesda, MD, USA).

2.6. Immunohistological analysis

In terms of immunohistological analysis, the femoral and intestinal sections were initially equilibrated in the 0.1 M Tris-buffered saline for 10 min. Then, after blocking with 10% normal goat serum in phosphate buffer saline (PBS) for an hour, the femoral sections were incubated overnight at 4 °C with primary antibodies against osteopontin (OPN) (dilution 1:50, Proteintech, 22952-1-AP, USA), osteoprotegerin (OPG) (dilution 1:200, Abcam, ab183910, USA), RANKL (dilution 1:200, Proteintech, 23408-1-AP, USA), TNF-α (dilution 1:200, Proteintech, 60291-1-Ig, USA), recombinant runt related transcription factor 2 (RUNX2) (dilution 1:200, Beyotime, AF2593, China). The intestinal sections were also incubated overnight at 4 °C with primary antibodies against Occludin (dilution 1:200, Proteintech, 27260-1-AP, USA), zonula occludens protein 1 (ZO-1) (dilution 1:200, Abcam, ab190085, USA), IL-1β

(dilution 1:50, Proteintech, 16806-1-AP, USA), and TNF-α (dilution 1:200, Proteintech, 60291-1-Ig, USA). After washing carefully in PBS for 15 min, the femoral and intestinal sections were incubated with horseradish peroxidase (HRP)-conjugated secondary antibodies (dilution 1:500, Servicebio, GB23303, China) for an hour at room temperature. 3,3′-diaminobenzidine (DAB) was used to visualize the OPN, OPG, RANKL, TNF-α, RUNX2, Occludin, ZO-1 and IL-1β. The positive signals were enumerated by the Image J software (National Institutes of Health, Bethesda, MD, USA) in six random and high-power fields (HPF) for the quantitative assessment.

2.7. Enzyme-linked immunosorbent assay (ELISA)

According to manufacturer's directions, serum 17β-Estradiol (E2) concentrations, the inflammation levels of IL-1β and TNF-α, and the levels of bone turnover markers, including OPG, RANKL and tartrate-resistant acid phosphatase 5B (TRACP5B) were measured using commercial ELISA kits (eBioscience, Shanghai, China).

2.8. Western blot analysis

In all groups of mice, the sections of colonic tissues were collected, and the total protein was further prepared in the lysis buffer (Beyotime, Shanghai, China) by lysing the tissue homogenates for an hour, and then centrifuged at 12,000 rpm and 4 °C for 10 min. Next, the protein assay kit (Beyotime, Shanghai, China) was applied to detect the protein content of supernatant, and the supernatant was collected and mixed with 5 × loading buffer. The crude proteins were heated for 10 min at 100 °C for denaturation. Then, the equal amounts of protein were separated using 12% sodium dodecyl sulfate-polyacrylamide gel electrophoresis (SDS-PAGE) and transferred onto the polyvinylidene difluoride (PVDF) membranes. Subsequently, after blocking with 5% non-fat skim milk in tris-buffered saline with 0.05% Tween-20 (TBST) for an hour, the membranes were incubated with primary antibodies against Occludin (dilution 1:1000, Proteintech, 27260-1-AP, USA), ZO-1 (dilution 1:500, Abcam, ab190085, USA), IL-1β (dilution 1:1000, Proteintech, 16806-1-AP, USA), and TNF-α (dilution 1:1000, Proteintech, 60291-1-Ig, USA) at 4 °C overnight. β-Actin (1:5000, Bioworld Technology, AP0060, USA) was applied as the internal control. Ultimately, after the membranes were washed for 10 min each of three times with TBST, membranes were then incubated with proper HRP-conjugated secondary antibodies (dilution 1:5000, Servicebio, GB23303, China) for 2 h at the room temperature. The blotted protein bands were visualized by enhanced chemiluminescence (ECL) detection kit (MilliporeSigma, Burlington, MA, USA), and the relative band intensities were then analyzed by Image J software (National Institutes of Health, Bethesda, MD, USA).

2.9. Fecal 16S rRNA sequencing and bioinformatics analysis

Fecal samples were freshly collected and stored at −80 °C before use. The HiPure Stool DNA Kits (Magen, Guangzhou, Guangdong, China) were used to extract the total DNA based on the manufacturer's instructions. The specific primers with barcode were used to amplify the samples DNA to enrich the bacterial 16S V3–V4 rRNA regions (V3: 341F, CCTACGGGNGGCWGCAG and V4: 806R, GGACTACHVGGGTATCTAAT). The polymerase chain reaction (PCR) amplification products were then recovered and quantified using QuantiFluorTM Quabit 3.0 (Thermo Fischer Scientific, Waltham, MA, USA) and ABI StepOnePlus Real-time PCR System (Life Technologies, Carlsbad, CA, USA). Subsequently, the purified amplified products were mixed in equal amounts and connected to the sequencing adapters to construct sequencing library. The established library was then sequenced on the HiSeq2500 system using the paired-end 250 (PE250) platform (Illumina, San Diego, CA, USA).

Furthermore, reads were filtered by the quantitative insights into microbial ecology (QIIME) quality filters [36]. Representative sequences were picked for each operational taxonomic unit (OTU), and the taxonomic information for each representative sequence was then annotated via the ribosomal database project (RDP) Classifier (version 2.2) [37]. In terms of the taxonomic classification, the tag reads were grouped into the OTUs at a sequence similarity level of 97% using Uparse software (version 9.2.64). Moreover, the taxonomic ranks, in descending order of size, were the domain, phylum, class, order, family, genus and species, and the differences between four groups of the samples were further identified. On this basis, the rarefaction analysis, α-diversity (including the ACE index, Chao1 index, Shannon index and Simpson index) and the rank abundance curve were calculated by QIIME software FLASH (version 1.2.11), Euclidean distance matrix and models (version 2.16.2) and Mothur (version 1.39.1). The β-diversity, including the principal coordinates analysis (PCoA) and the non-metric multi-dimensional scaling (NMDS) were conducted in accordance with the abundance of OTUs by the R packages GUniFrac (version 1.0) and Muscle (version 3.8.31). The linear discriminant analysis effect size (LEfSe, version 1.0) was conducted to identify the significant differences between four groups [38]. Ultimately, the PICRUSt software was also used to conduct the targeted community function prediction analysis, combining kyoto encyclopedia of genes and genomes (KEGG) pathways information of genes to predict the pathway status of the overall community.

2.10. Fecal short chain fatty acids (SCFAs) detection

The SCFAs in the feces of all groups were detected in accordance with the methods previously described by Chen et al. [39]. Briefly, the appropriate amount of feces was extracted and mixed with 5 times volume of water by vortexing and centrifuging, and the supernatant was mixed with one-tenth of the volume of formic acid. Then, the mixed solution was filtrated through a 0.45 μm microporous membrane, and the filtrate was injected into a gas chromatograph (Agilent 7820A, Palo Alto, CA, USA). The SCFAs were then separated using a fused silica capillary column (Agilent, Palo Alto, CA, USA), with the injection temperature at 240 °C and the ion source temperature at 200 °C. The helium was used as the carrier gas with a constant blow rate of 1 ml/min, and an injection volume of 1 μl without shunting. Furthermore, the column temperature program started at 50 °C and increased to 120 °C at a rate of 15 °C/min, then increased to 170 °C at a rate of 5 °C/min, then increased to 210 °C at a rate of 15 °C/min, and ultimately held at 210 °C for 3 min. The peak areas of target compounds were quantified, and the standard curves of the acetic acid, propionic acid, iso-butyric acid, butyric acid, iso-valeric acid, valeric acid and caproic acid were analyzed and obtained.

2.11. Statistical analysis

The overall quantified data in this current study were analyzed by GraphPad Prism 8 software (GraphPad, San Diego, CA, USA) and presented as the form of mean ± standard deviation (SD). Moreover, the statistical differences were analyzed by the one-way ANOVA followed by Tukey test, and the Pearson's correlation was used to make the comparisons between groups. P value < 0.05 was regarded as statistically significant. Each experiment consisted of at least three replicates.

3. Results

3.1. Effects of FMT treatment on the body weight and serum E2 concentrations in mice with OVX-induced OP

As exhibited in Fig. 1C–E, the mice in OVX group and OVX + NS group gained more weight than the mice in Sham group, and the serum E2 concentrations of mice in OVX group, OVX + NS group and OVX +

FMT group were significantly lower than that in Sham group. After the FMT treatment, the body weight of mice in OVX + FMT group significantly reduced (compared with the mice in OVX group and OVX + NS group), and there was no significant difference in weight gain between the mice in OVX + FMT group and Sham group.

3.2. FMT treatment prevented the bone loss in mice with OVX-induced OP

In order to investigate the effects of FMT treatment on bone loss in the mice with OVX-induced OP, the bacterial suspension was transplanted to the recipient mice by gavage. The effects of FMT treatment on the structure of distal femur trabecular bone were analyzed by Micro-CT (Fig. 2A) and the femoral HE staining indicated a reduced trabecular bone area of the mice in OVX group and OVX + NS group, and retention in the distal femur of mice in OVX + FMT group (Fig. 2B). Moreover, FMT treatment significantly increased the distal femoral BMD, BS/TV, BV/TV, Tb.N and Tb.Th, and decreased the Tb.Sp relative to OVX group (Fig. 2C–H).

As for the immunohistological analysis, the results suggested that the expressions of OPN, RUNX2 and OPG decreased after OVX, and FMT treatment enhanced the expressions of OPN, RUNX2 and OPG relative to that in OVX group and OVX + NS group (Fig. 3A–F). Meanwhile, the results demonstrated that the expression of RANKL enhanced after OVX, and FMT treatment decreased the expression of RANKL relative to that in OVX group and OVX + NS group (Fig. 4A, D). TRAP staining also showed the apparent enhancement in the total number of $TRAP^{+}$ osteoclasts along the trabecular bone in mice with OVX-induced OP, whereas FMT treatment decreased the number of $TRAP^{+}$ osteoclasts per bone surface area (Fig. 4B, E). In addition, the expression of TNF-α was also measured in the femoral tissue, and the results revealed the enhanced expression of TNF-α in mice with OVX-induced OP, whereas the FMT treatment decreased the expression of TNF-α in the femoral tissue (Fig. 4C, F). Furthermore, the serum bone turnover markers were also measured, and the results indicated that the mice in OVX + FMT group exhibited a declined trend in the levels of RANKL and TRACP5B (Fig. 4G–H), and an increased tendency in the level of OPG (Fig. 3G). Collectively, these data revealed that FMT treatment was able to prevent the bone loss in the mice with OVX-induced OP, and FMT treatment might be involved in the bone regulation by inhibiting the levels of pro-osteoclastogenic cytokines, so as to further decrease bone resorption and increase bone formation.

3.3. FMT treatment maintained the integrity of intestinal barrier in mice with OVX-induced OP

Next, in order to explore the effects of FMT on the integrity of intestinal barrier in mice with OVX-induced OP, we conducted the further exploration. On one hand, as shown in Fig. 5A, the colon HE staining suggested that the intestinal cavity of the mice with OVX-induced OP was relatively sparse and the intestinal gap was significantly enlarged. After FMT treatment, the mice in OVX + FMT group and Sham group exhibited similar but not equivalent result in terms of the integrity of intestinal barrier. On the other hand, as demonstrated by the results of immunohistological analysis and western blot analysis (Fig. 5B–H), the expressions of Occludin and ZO-1 were relatively low in OVX group, which may result in high intestinal permeability. However, after FMT treatment, the mice in OVX + FMT group exhibited higher expressions of tight junction proteins (Occludin and ZO-1). In general, these results suggested that OVX-induced OP can jeopardize the integrity of intestinal barrier and increase the intestinal permeability, while FMT treatment was able to restore the integrity of intestinal barrier and decrease the intestinal permeability.

3.4. FMT treatment inhibited the OVX-induced inflammation

Furthermore, in order to further investigate the effects of FMT on inflammation, we assessed the changes in intestinal and humoral pro-osteoclastogenic cytokines. As demonstrated by the results of immunohistological analysis and western blot analysis (Fig. 6A–G), the expressions of IL-1β and TNF-α increased after the OVX-induced OP, which was suppressed by FMT treatment. After FMT treatment, the mice in OVX + FMT group and Sham group exhibited similar but not equivalent result in terms of the intestinal inflammation. Consistently, compared with Sham group, the results revealed that OVX augmented the serum concentrations of TNF-α and IL-1β, and FMT treatment was able to defy this augment of pro-osteoclastogenic cytokines (Fig. 6H–I).

3.5. FMT treatment modulated the imbalance of GM in mice with OVX-induced OP

Subsequently, in order to examine whether FMT had modulated GM, we conducted 16S V3–V4 rRNA regions sequencing to analyze the bacterial taxonomic composition following the FMT treatment in the mice with OVX-induced OP. As for the α-diversity, significant differences were existed in the ACE and Chao1 indexes between the Sham group and OVX group (Fig. 7A–B), which suggested that OVX-induced OP may have a marked influence on the richness of microbiota. After the FMT treatment, the mice in OVX + FMT group and Sham group exhibited similar but not equivalent result in terms of the richness of microbiota. Moreover, the rank abundance curve revealed the consistent results (Fig. S1A). However, no significant difference was observed in terms of the Shannon and Simpson indexes (Fig. 7C–D). Furthermore, in order to detect the degree of similarity between the different microbial communities, the β-diversity was analyzed by the means of PCoA and NMDS. As exhibited in Fig. 7E–F, PCoA and NMDS showed a distinct clustering of the microbiota composition for each group and revealed that the microbial communities of mice in OVX group were significantly different from that in Sham group and OVX + FMT group, which suggested that FMT treatment improved the OVX-induced OP possibly by modulating the imbalance of GM.

Next, in order to evaluate the specific changes of GM, the relative abundance (top 10) of predominant taxa was further analyzed in this study (Figs. S1B–D). At the phylum level, *Cyanobacteria*, *Actinobacteria*, *Proteobacteria*, *Firmicutes* and *Bacteroidetes* exhibited significant differences among different four groups (Fig. S1B). At the class level, the content of *Bacteroidia* was decreased and the content of *Melainabacteria* was increased in OVX group, while FMT treatment regained this imbalance (Fig. S1C). At the order level, the microbiota of four groups was mainly dominated by *Bacteroidales*, *Clostridiales*, *Erysipelotrichales*, *Lactobacillales* and *Gastranaerophilales* (Fig. S1D). Furthermore, in order to identify the bacterial taxonomic markers relevant to OVX-induced OP, the LEfSe analysis was further conducted and presented in Fig. 7G. The cladogram was further generated and the significant differences in bacterial taxonomic composition were occurred in the different four group (Fig. 7H.). In OVX + FMT group, *s_unclutured_bacterium_f_Prevotellaceae*, *g_unclutured_bacterium_f_Prevotellaceae*, *s_unclutured_bacterium_f_Lachnospiraceae*, *f_Lachnospiraceae*, *f_Ruminococcaceae*, *g_unclutured_bacterium_f_Lachnospiraceae* were identified. Collectively, these data indicated that FMT treatment could modulate the GM in mice with OVX-induced OP. Furthermore, the species phylogenetic tree and species correlation network were also exhibited in Figs. S1E–F.

3.6. The prediction of potential metabolic functions of GM

Moreover, in accordance with the changes of GM among these groups, we further used PICRUSt to predict the potential metabolic functions of GM, and also inferred the functional contents of metagenome. As shown in Fig. S2A, the functional contribution of bacteria was predicted through the compositions and difference analysis of KEGG metabolic pathways, and the comparisons between OVX + FMT group and other groups was also exhibited in Figs. S2B–D. Specifically, most of the results were enriched in terms of metabolism, including global and overview maps, carbohydrate metabolism, energy metabolism, amino acid metabolism,

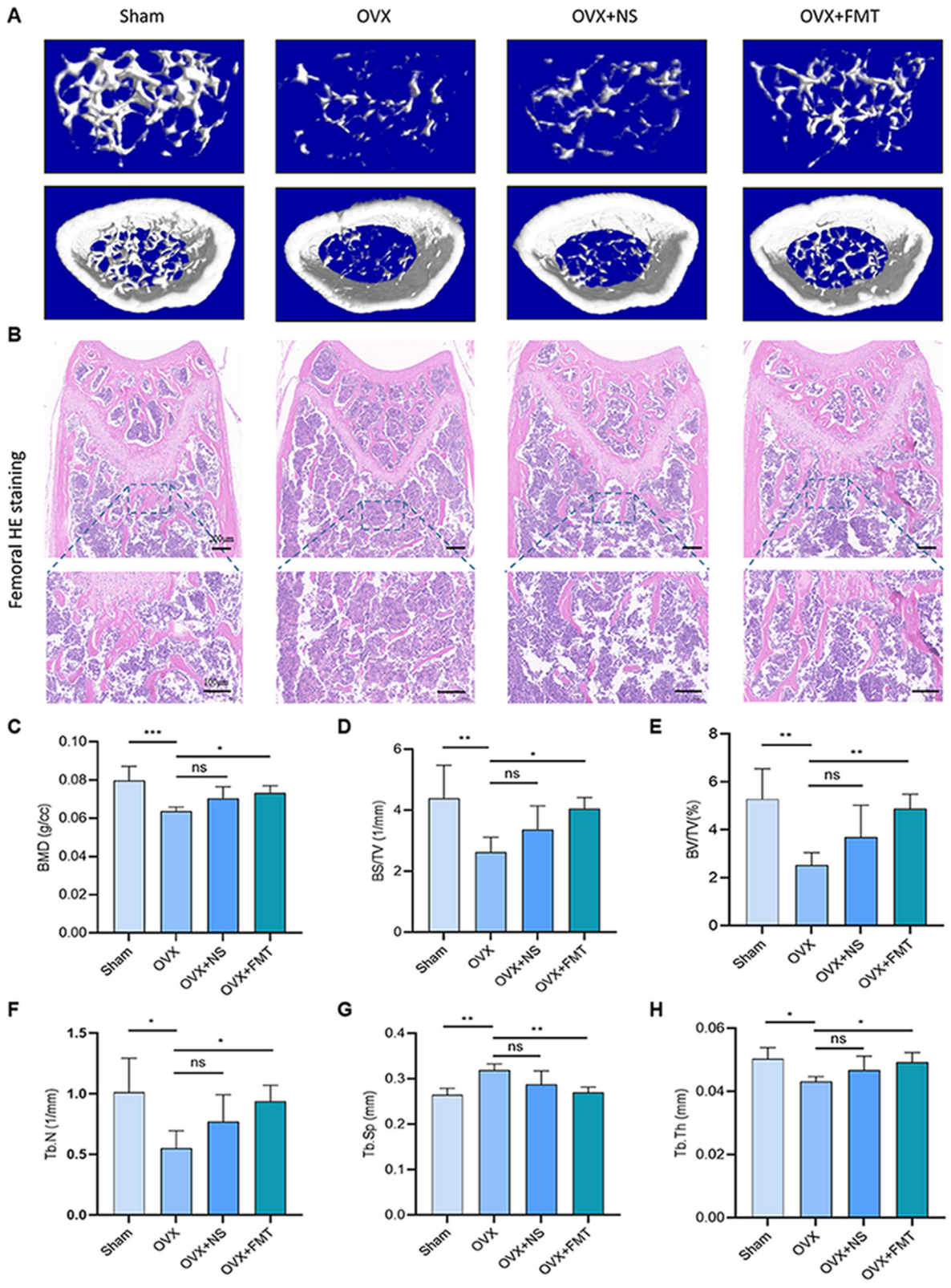

Figure 2. FMT treatment prevented the bone loss in mice with OVX-induced OP. (A) The Micro-CT images of the structures of distal femur trabecular bone (B) HE staining of the trabecular bone area. Scale bars represented 200 μm and 100 μm; (C) BMD (D) BS/TV, (E) BV/TV (F) Tb.N, (G) Tb.Sp and (H) Tb.Th on the distal femur trabecular bone were analyzed by the Micro-CT. Data were expressed as mean ± SD ($n = 5$). One-way ANOVA procedure followed by the Tukey test and Pearson's correlation were used to assess statistical significance. The different letters represented significant differences between the different groups, $^{*}P < 0.05$, $^{**}P < 0.01$, and $^{***}P < 0.001$ compared with the corresponding group.

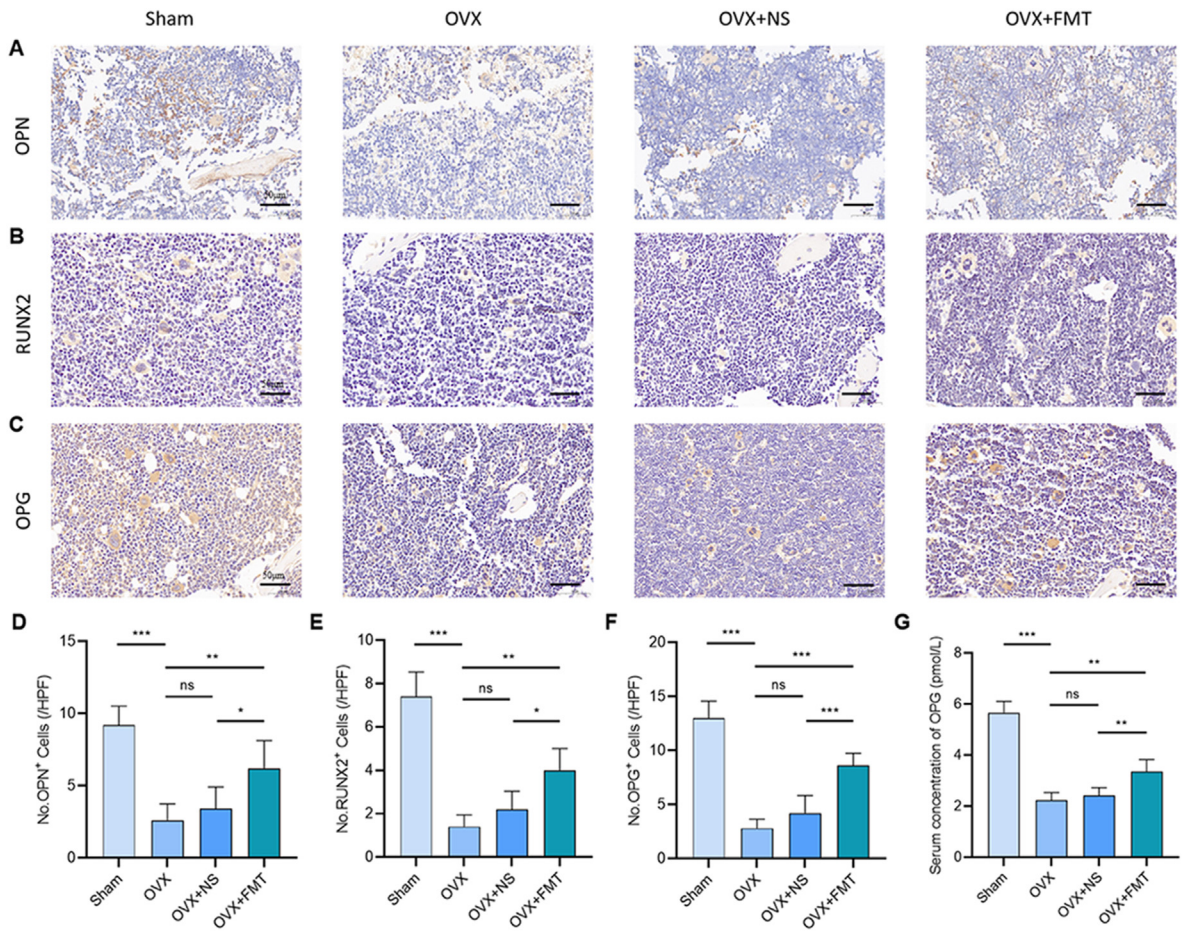

Figure 3. FMT treatment promoted osteogenesis. (A) OPN (B) RUNX2, and (C) OPG stained the sections of distal femur. Scale bars represented 50 μm; (D) No. OPN^+ cells (E) No. $RUNX2^+$ cells; (F) No. OPG^+ cells (G) The serum concentration of OPG. Data were expressed as the mean ± SD ($n = 5$). One-way ANOVA procedure followed by the Tukey test and Pearson's correlation were used to assess statistical significance. The different letters represented significant differences between different groups, $^*P < 0.05$, $^{**}P < 0.01$, and $^{***}P < 0.001$ compared with corresponding group.

nucleotide metabolism, endocrine system, metabolism of cofactors and vitamins, lipid metabolism, and so on. Notably, the terms of the replication and repair, infectious diseases: bacterial, membrane transport, cell motility, drug resistance: antimicrobial, cellular community-prokaryotes, and signal transduction in OVX + FMT group were significantly different with those of OVX group and OVX + NS group.

3.7. FMT treatment restored the fecal SCFAs in mice with OVX-induced OP

Based on the above findings, it was acknowledged that FMT treatment could modulate the GM in mice with OVX-induced OP and the potential metabolic functions were synchronously predicted. Moreover, as one of the most significant metabolites of GM, the SCFAs were the effective regulators of osteoclast metabolism and bone homeostasis, and also played a critical role in the prevention and treatment of systemic metabolic diseases. Thus, we detected the contents of fecal SCFAs to further explore the potential mechanisms of FMT treatment against PMOP. Specifically, the QC overlapping chromatogram was shown in Fig. 8A to evaluate the stability of evaluation method. As exhibited in Fig. 8B, the acetic acid, propionic acid and butyric acid were the main fermentation products in the feces of mice in all groups, and the contents of acetic acid, propionic acid and total acids of the mice in OVX + FMT group were significantly higher than those of mice in OVX group. However, no significant difference was observed in terms of butyric acid. Taken together, the total acids, especially the acetic acid and propionic acid in the feces of mice with OVX-induced OP decreased significantly, while enhanced significantly after the FMT treatment.

Furthermore, Fig. 8C–E exhibited the orthogonal partial least squares discriminant analysis (OPLS-DA) between the OVX + FMT group and other groups, and it was also intuitively observed that the fecal samples of mice in OVX + FMT group were more clustered and less discrete than those in OVX group and OVX + NS group (Fig. 8D–E). Notably, we also observed that the mice in OVX + FMT group and Sham group exhibited similar but not equivalent result (Fig. 8C). Moreover, Fig. 8F–H showed the correlation analysis of differential metabolites between OVX + FMT group and other groups, which revealed that there were significant differences in the consistency of the variation trends of metabolites in the feces of mice between OVX + FMT group and other groups. On the basis of obtaining differential metabolites, we further used receiver operating characteristic (ROC) curve to assess and screen potential biomarkers between the OVX + FMT group and other groups, and the relevant results were presented in Fig. S3.

4. Discussion

With the prolongation of the life-span of global population and growing number of elderly individuals, the burden caused by OP and osteoporotic fractures is increasingly heavy-laden [40]. As an indispensable part of OP, the bone health and PMOP of middle-aged and elderly women is of particular concern [41]. Currently, accumulating evidence suggests that GM dysbiosis is involved in the pathogenesis and clinical manifestations of PMOP [19,42]. In this current study, our data suggested that FMT treatment could reshape the status of GM and ameliorate the bone loss in mice with OVX-induced OP. The relevant

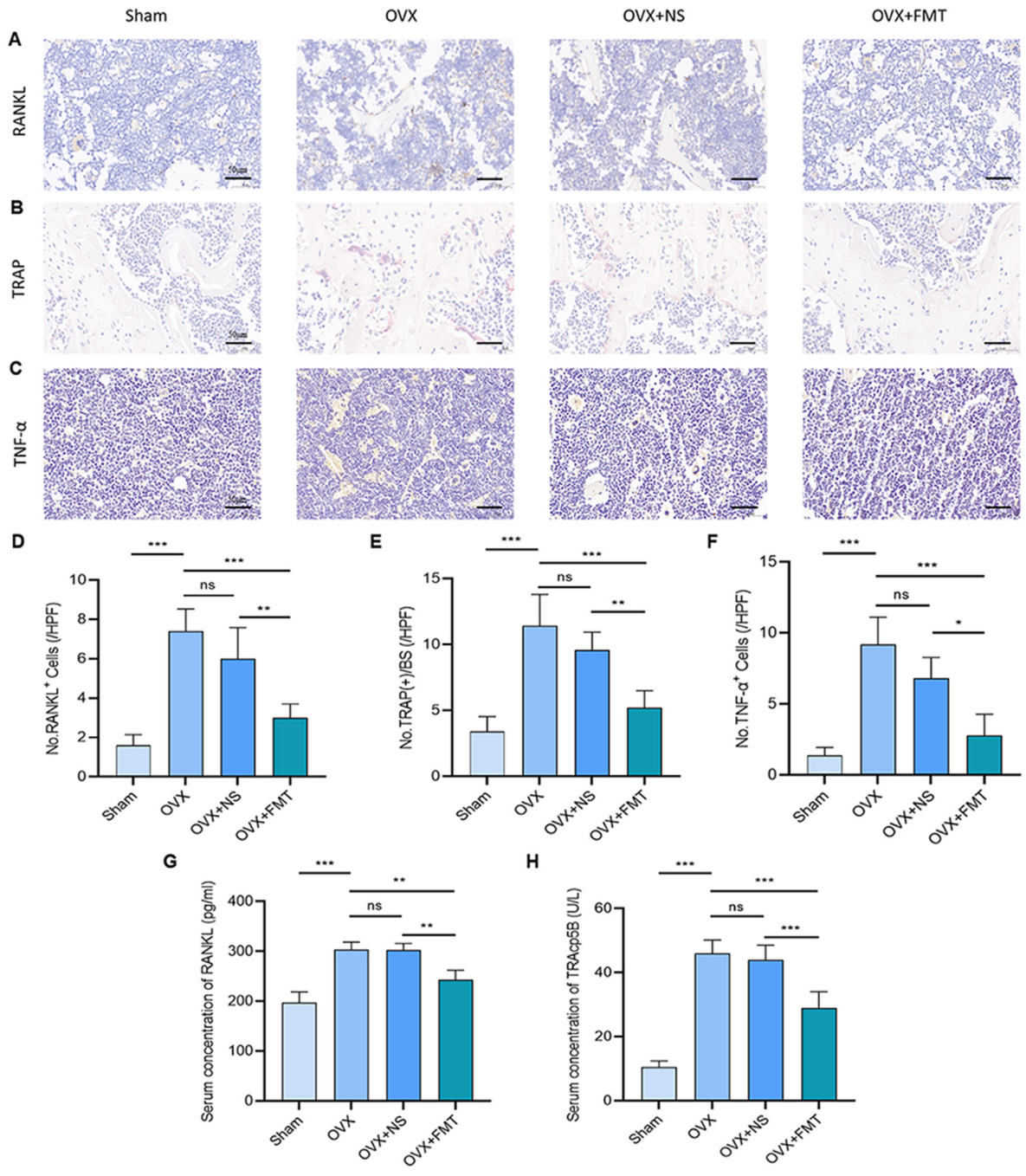

Figure 4. FMT treatment suppressed osteoclastogenesis. (A) RANKL (B) TRAP, and (C) TNF-α stained the sections of distal femur. Scale bars represented 50 μm; (D) No. RANKL^{+} cells (E) No. TRAP^{+} cells; (F) No. TNF-α^{+} cells (G) Serum concentration of RANKL; (H) The serum concentration of TRACP5B. Data were expressed as mean ± SD ($n = 5$). One-way ANOVA procedure followed by the Tukey test and Pearson's correlation were used to assess statistical significance. The different letters represented significant differences between different groups, $^{*}P < 0.05$, $^{**}P < 0.01$, and $^{***}P < 0.001$ compared with the corresponding group.

mechanism was to inhibit excessive osteoclastogenesis by correcting the imbalance of GM, improving the fecal SCFAs level, optimizing the intestinal permeability, and suppressing the release of pro-osteoclastogenic cytokines. During this process, the blood circulation also provided a bridge between pro-osteoclastogenic cytokines, GM, SCFAs and bone. Meanwhile, the overall experimental flow chart and mechanism patterns were presented in Fig. 9. Hence, on this basis, FMT treatment may be an alternative option to serve as a promising candidate for the prevention and treatment of PMOP in the future.

As a newly emerging treatment approach in recent years, FMT mainly refers to the transplantation of bacteria from healthy donors to GM dysregulated recipients, with the purpose of restoring intestinal microbial homeostasis and improving GM dysbiosis [22]. Currently, FMT is gradually applied to the treatment of numerous diseases, while there is still no relevant report on the treatment of PMOP, and there are also no standardized treatment strategies for FMT [23]. Nevertheless, the effects of FMT on mineral metabolism have been gradually proceed and observed in an orderly way. With regard to this, Sjögren et al. [17] suggested that compared with the normal mice, the bone mass of germ-free (GF) mice increased and the CD4+T cells in bone marrow and the level of TNF-α decreased, while the bone mass, CD4+T cells and level of TNF-α of GF mice returned to normal after the transplantation of bacteria from normal mice. Schepper et al. [43] transplanted the bacteria of glucocorticoid-induced osteoporosis (GIO) mice to the mice treated

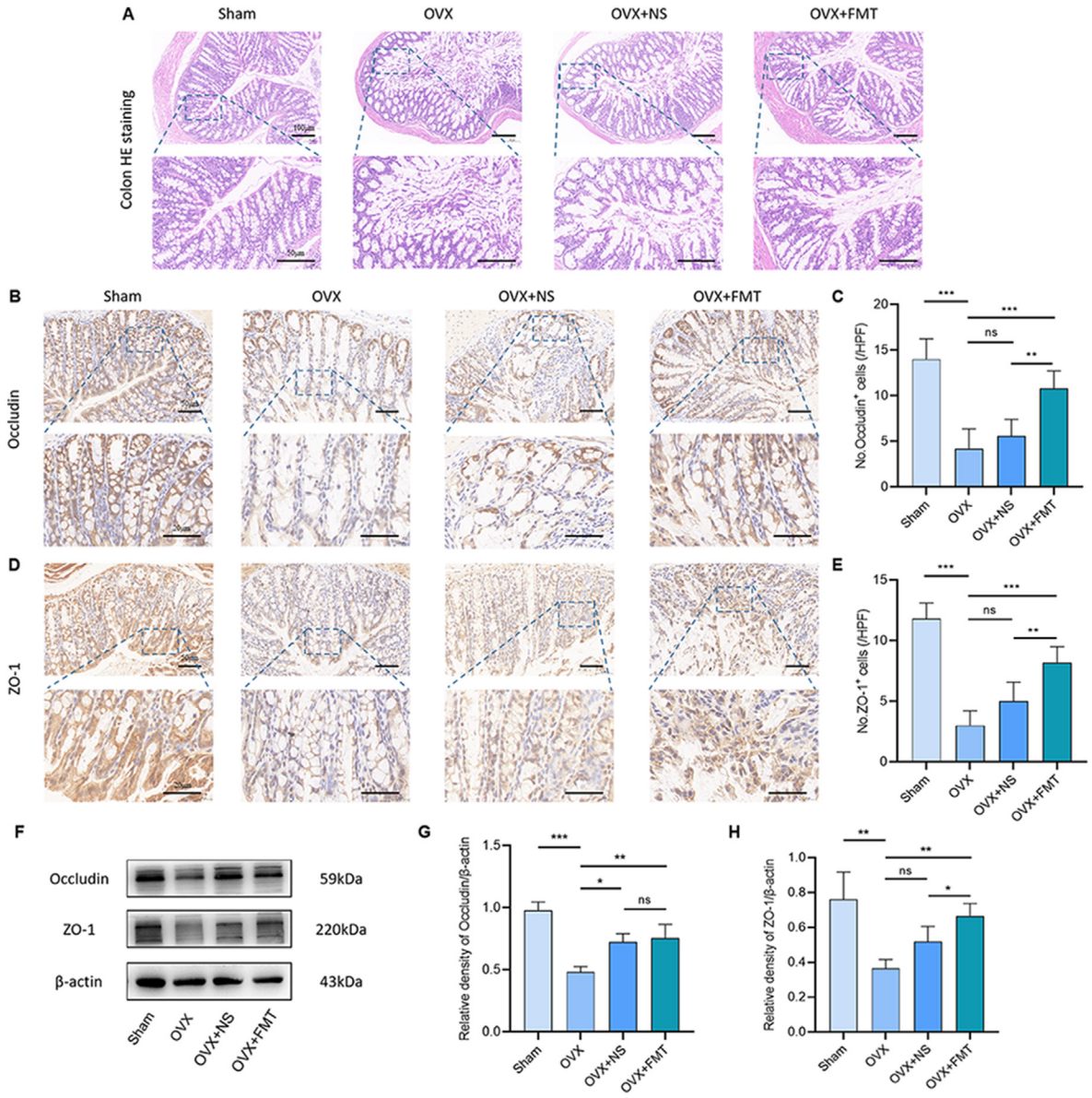

Figure 5. FMT treatment maintained the integrity of intestinal barrier in the mice with OVX-induced OP. (A) HE staining of colonic tissues. Scale bars represented 100 μm and 50 μm (B) Occludin and (D) ZO-1 stained the sections of colonic tissue. Scale bars represented 50 μm and 20 μm; (C) No. Occludin^{+} cells (E) No. ZO-1^{+} cells; (F–H) The representative western blots and the quantifications of Occludin and ZO-1. Data were expressed as mean ± SD ($n = 5$). One-way ANOVA procedure followed by the Tukey test and Pearson's correlation were used to assess statistical significance. The different letters represented significant differences between the different groups, *$P < 0.05$, **$P < 0.01$, and ***$P < 0.001$ compared with the corresponding group.

with antibiotics for one week, and observed that the bone mass of recipient mice decreased, indicating that the effects of glucocorticoid on bone mass were able to be transferred by FMT. Ma et al. [44] also revealed that the GM transplanted from young rats could alleviate the bone loss in aged rats with senile osteoporosis by improving the composition of GM and function of intestinal mucosal barrier. Wang et al. [45] also revealed that GM dysbiosis by transferring the feces from senile osteoporotic rats to young rats can induce OP, and the changed GM and impaired intestinal mucosal barrier contributed to the pathogenesis of OP. Collectively, these relevant studies have jointly exhibited the potential bone protective effects of FMT, which demonstrates its application value in protecting bone mass and regulating bone metabolism. Herein, we applied the FMT treatment to OVX mice that mimicked post-menopausal estrogen-deficiency, and indicated that FMT treatment might intervene the bone loss via the GM-bone axis.

In addition, on one hand, it was demonstrated that estrogen-deficiency was related to the intestinal mucosal barrier disruption and was able to undermine various kinds of bone properties through the modulation of GM-bone axis [46,47]. On the other hand, PMOP is intimately relevant to the systemic chronic inflammation and accompanied with the augment of various kinds of pro-osteoclastogenic cytokines (including TNF-α, IL-1β, IL-6 and so on), which acts as the stimulators of osteoclastogenesis and plays a crucial role in the process of osteoclast overgeneration [48,49]. With regard to this, the function of intestinal mucosal barrier is critical for maintaining systemic inflammatory responses. After the intestinal mucosal barrier is damaged, the “inflamed and leaky gut” may cause the bacterial translocation and toxin invasion, which further results in the intestinal inflammatory response [50]. Meanwhile, the tight barriers are mainly formed by tight junction proteins between epithelial cells (involving Claudin family of proteins, ZO-1 and Occludin) to selectively restrict the diffusion of luminal toxins and antigens through mucous membranes [51]. In this current study, our data

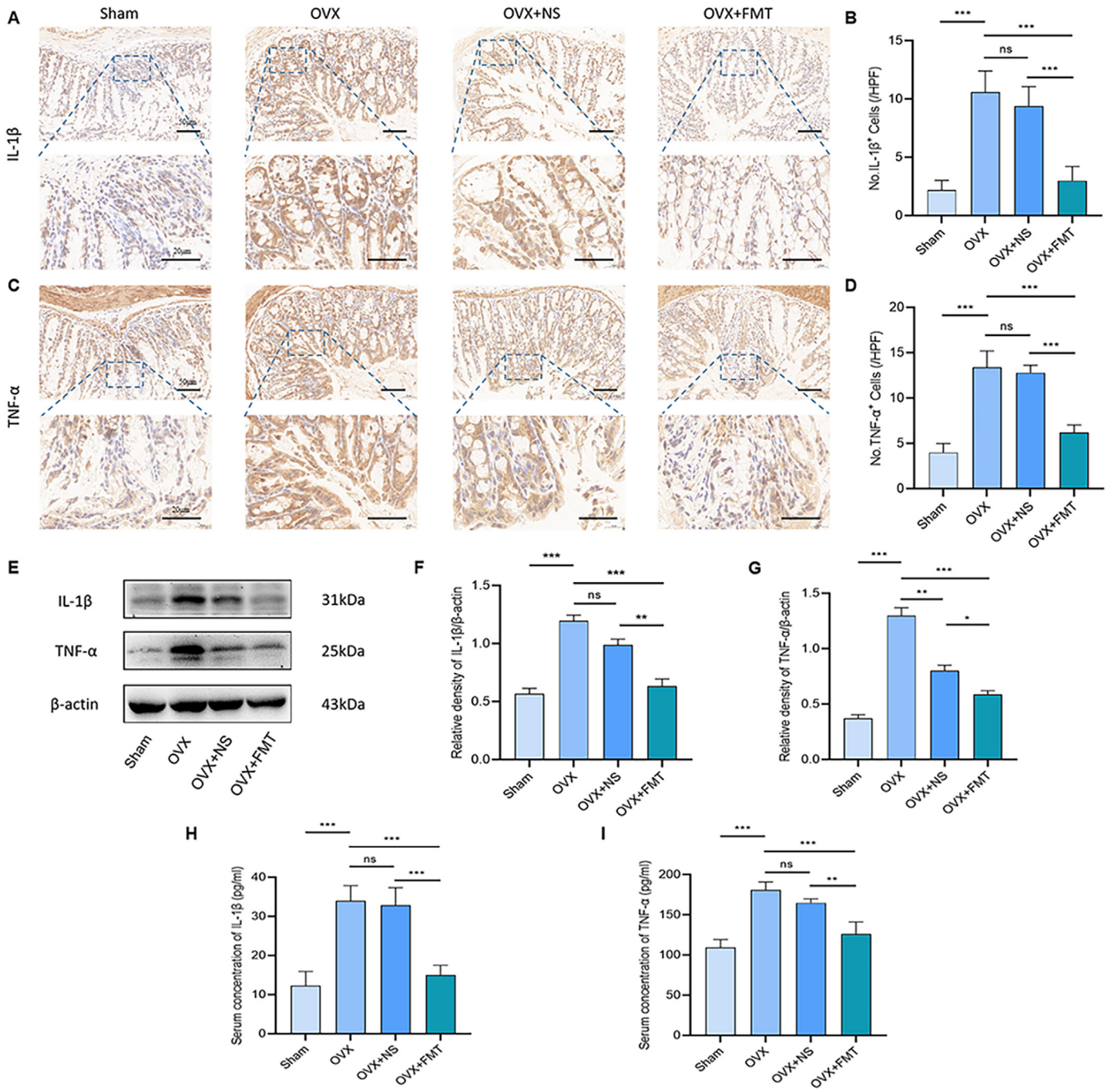

Figure 6. FMT treatment inhibited the OVX-induced inflammation. (A) IL-1β and (C) TNF-α stained the sections of colonic tissues. Scale bars represented 50 μm and 20 μm; (B) No. IL-1β^{+} cells (D) No. TNF-α^{+} cells; (E–G) The representative western blots and the quantifications of IL-1β and TNF-α (H) The serum concentration of IL-1β; (I) The serum concentration of TNF-α. Data were expressed as mean ± SD ($n = 5$). One-way ANOVA procedure followed by the Tukey test and Pearson's correlation were used to assess statistical significance. Different letters represented the significant differences between the different groups, $^{*}P < 0.05$, $^{**}P < 0.01$, and $^{***}P < 0.001$ compared with the corresponding group.

showed that intestinal permeability enhanced after estrogen withdrawal, which might be a vital factor for the augment of pro-osteoclastogenic cytokines after the estrogen-deficiency. Intriguingly, we observed that FMT treatment restored the decline of expressions of tight junction proteins (ZO-1 and Occludin), which guarded the intestinal mucosal barrier, caused a lower intestinal permeability, and then reduced the release of pro-osteoclastogenic cytokines (IL-1β and TNF-α). As a result, it is recognized that the gut is a non-negligible and particularly significant source of pro-osteoclastogenic cytokines after the estrogen-deficiency, and it is also promising to proceed from the perspective of gut for further intervention and treatment of PMOP.

Numerous previous studies have indicated that GM dysbiosis might occur in the PMOP patients and OVX-induced murine models. van den Heuvel et al. [52] observed in a population-based study that the supplementation of *Transgalactooligosaccharides* could enhance the intestinal calcium absorption of postmenopausal women, so as to further protect their bones. Collins et al. [53] revealed that when the OVX-induced mice were fed with *Lactobacillus reuteri*, the intestinal permeability of mice can

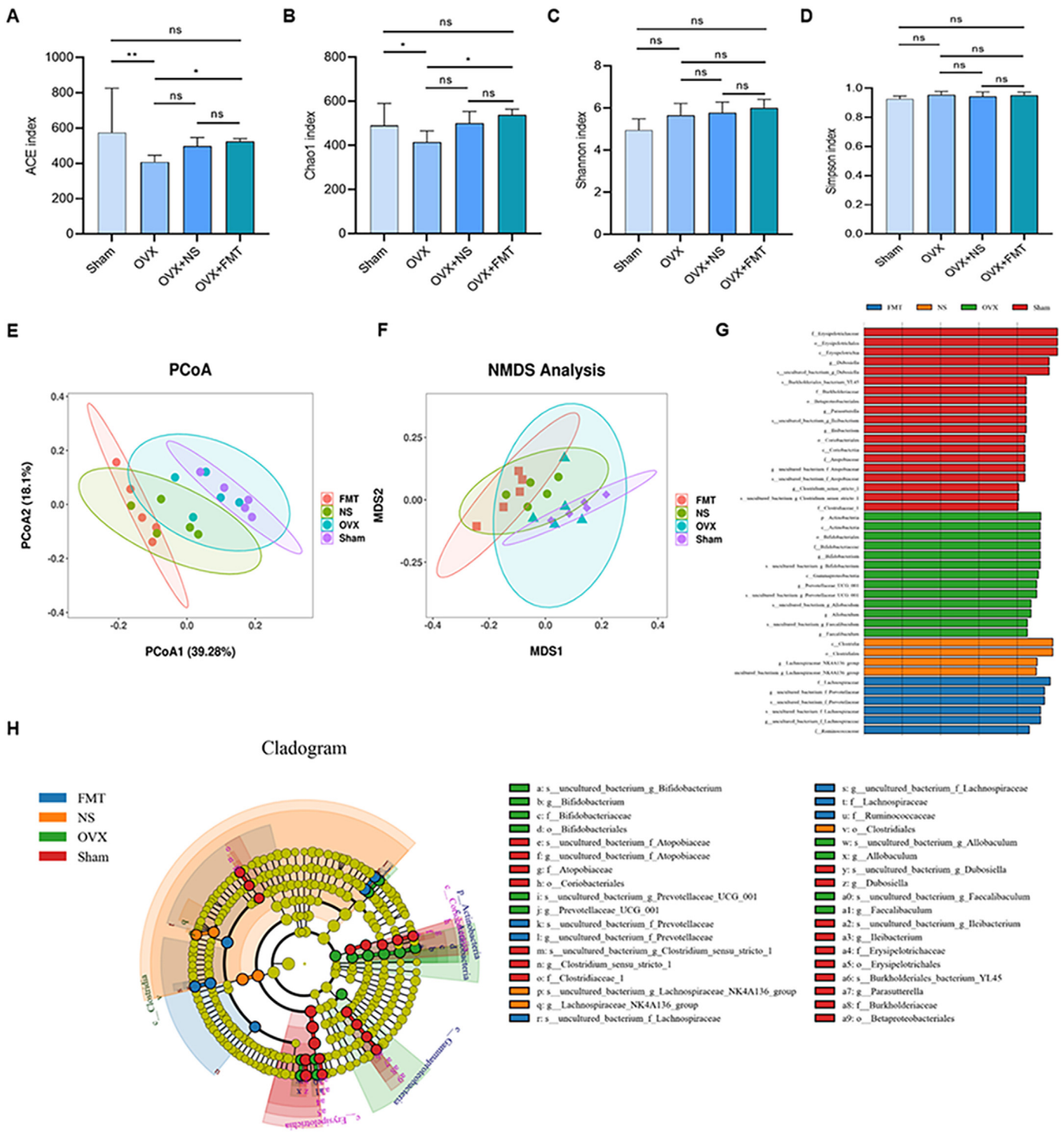

Figure 7. FMT treatment modulated the imbalance of GM in mice with OVX-induced OP. (A) ACE index (B) Chao1 index; (C) Shannon index (D) Simpson index; (E) PCoA plots (F) NMDS analysis plots; (G) Histogram of LDA value distribution (H) Evolutionary branching diagram of LEfSe analysis. Data were expressed as mean ± SD ($n = 5$). The one-way ANOVA procedure followed by the Tukey test and Pearson's correlation were used to assess statistical significance. The different letters represented significant differences between different groups, $^{*}P < 0.05$, $^{**}P < 0.01$, and $^{***}P < 0.001$ compared with the corresponding group.

be reduced, and bone loss caused by OVX can be delayed. In this study, we were committed to investigating whether FMT can act as an interventional method to prevent the PMOP, and if so, what specific components of FMT played a critical role in this process. By utilizing the gold-standard OVX-induced mice models and further conducting 16S rRNA sequencing, we found that *Prevotellaceae*, *Lachnospiraceae* and *Ruminococcaceae* may participate in the correction of OVX-induced GM dysbiosis and act as the vital components in the process of FMT. In addition, the homeostasis is tended to be maintained under healthy conditions via the interactions between intestinal mucosal barrier, GM, inhibition of intestinal pathogens, and systemic inflammatory system [54]. As for postmenopausal women, estrogen-deficiency may alter the overall composition and structure of GM, resulting in the decline of microbial diversity [55,56]. The intestinal pathogens may invade into host

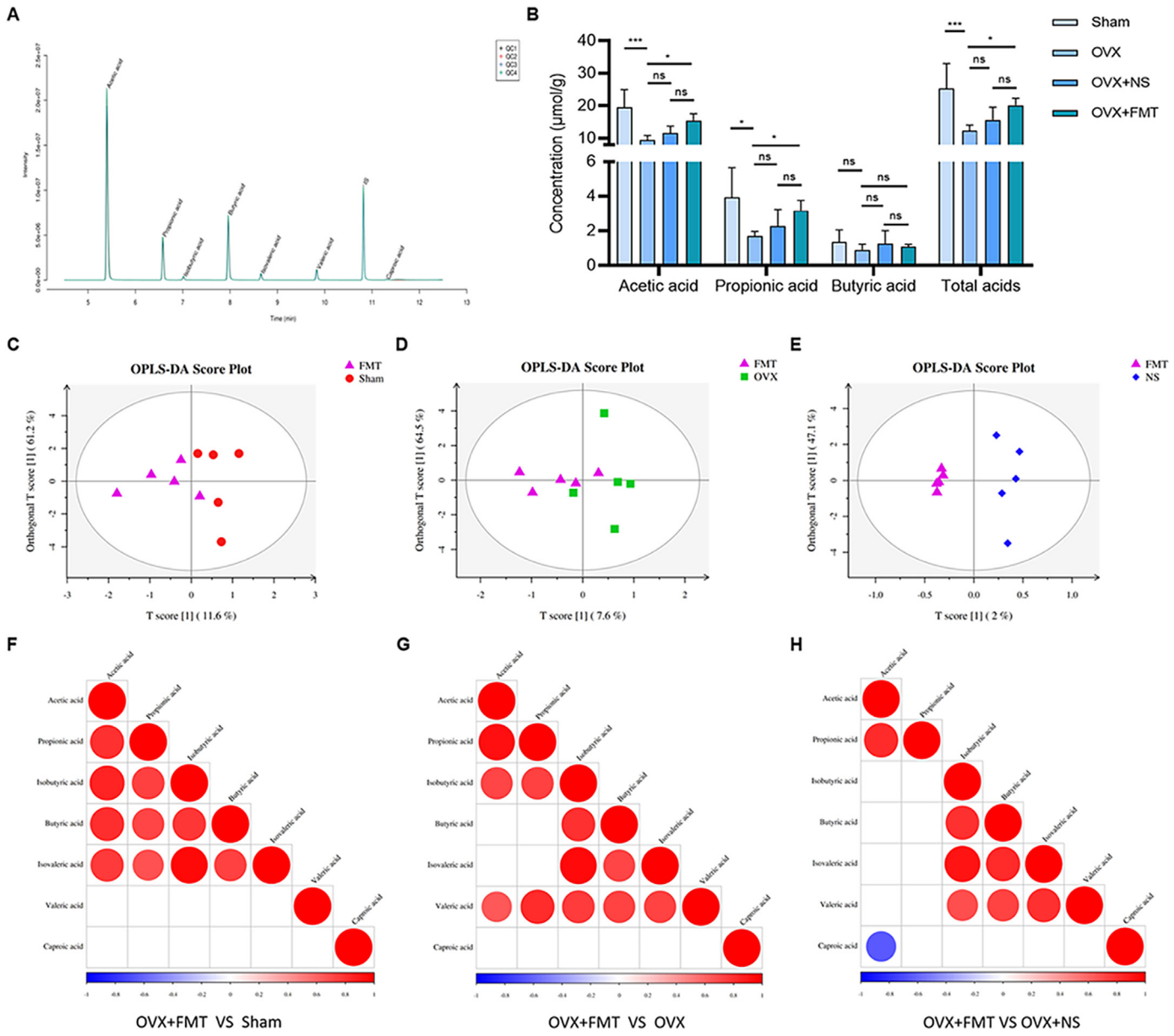

Figure 8. FMT treatment restored the fecal SCFAs in mice with OVX-induced OP. (A) QC overlapping chromatogram (B) The contents of acetic acid, propionic acid, butyric acid and total acids in the feces of mice in all groups; (C–E) The OPLS-DA analysis plots between the OVX + FMT group and other groups (F–H) The correlation analysis of differential metabolites between the OVX + FMT group and other groups. Data were expressed as mean ± SD ($n = 5$). One-way ANOVA procedure followed by the Tukey test and Pearson's correlation were used to assess statistical significance. The different letters represented significant differences between the different groups, $^{*}P < 0.05$, $^{**}P < 0.01$, and $^{***}P < 0.001$ compared with corresponding group.

with impaired intestinal mucosal barrier and trigger an inflammatory response, which ultimately promotes the bone absorption and persistent bone loss [57,58]. Herein, after FMT intervention, the mice in OVX + FMT group and OVX group showed the significant differences of α-diversity and β-diversity, and the mice in OVX + FMT group and Sham group also exhibited similar but not equivalent result in terms of richness of microbiota. Taken together, the intestinal mucosal barrier, GM, SCFAs and the inflammatory system are inseparable and interrelated, and changes in one of them may induce changes of other systems.

Furthermore, SCFAs, as one of the significant components of intestinal metabolites, are mainly consisted of the carboxylic acids and small hydrocarbon chains, and can be produced by intestinal symbiotic bacteria via fermenting the indigestible carbohydrates in foods [59,60]. Clinical data revealed that SCFAs were able to be regarded as a bridge to promote the bone formation and inhibit the bone absorption, thus improving the bone mass and bone strength [61]. Besides, Kim et al. [62] showed that SCFAs could enhance the solubility of minerals in intestinal tract by lowering the PH value of intestine, so as to enable the calcium easier to be absorbed by body and further improve bone mass. By supplementing SCFAs to the antibiotic treated mice, Yan et al. [63] also observed that the serum level of insulin-like growth factor-1 (IGF-1) and bone mass can be restored to a similar level as that of the non-antibiotic treated mice, indicating that SCFAs can indirectly participate in the regulation of bone mass by influencing the level of IGF-1. Herein, our data suggested that the declining contents of SCFAs in the feces of mice in OVX group were related to the augment of inflammatory levels in the gut. Meanwhile, it was also observed the lower levels of inflammatory parameters (IL-1β and TNF-α) in the intestine and higher contents of fecal SCFAs after the FMT treatment. Hence, it was recognized that FMT treatment may play a role in bone protection by up-regulating the

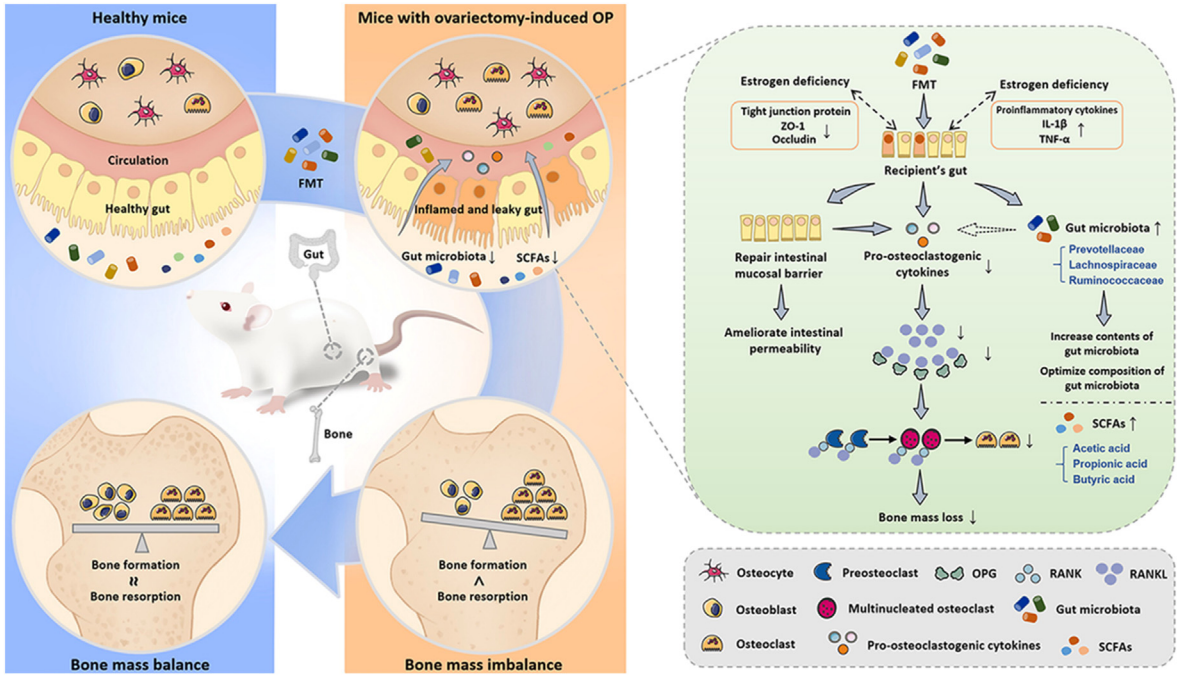

Figure 9. Graphic abstract and overall experimental flow chart and mechanism patterns. Estrogen-deficiency disrupted the intestinal mucosal barrier, and interaction between the GM, SCFAs and host inflammatory system altered accordingly. Based on this, FMT inhibited the excessive osteoclastogenesis and prevented the bone loss by correcting the GM imbalance, improving the fecal SCFAs level, optimizing the intestinal permeability and suppressing release of pro-osteoclastogenic cytokines, which may be an alternative option to serve as a promising candidate for the prevention and treatment of PMOP in the future.

contents of SCFAs and suppressing the persistent inflammation.

In general, the strong point of our current study was to explore the crosstalk effects based on GM-bone axis in PMOP, and analyzed the differences and changes at different levels of the mice in each group before and after FMT treatment by combining the 16S rRNA sequencing and metabolomics. However, it is still essential to recognize and state certain shortcomings. On one hand, numerous studies have shown that there are certain minor and transient adverse effects after FMT treatment (mainly including abdominal discomfort, nausea, vomiting, bloating, flatulence, and so on) [64–67]. The security of FMT has not been fully and clearly explained, which still needs to be verified by animal experiments and human prospective trials with the larger sample sizes in the future. On the other hand, in most existing microbial-related studies, the analysis of microbiomes mainly depends on the 16S rRNA sequencing technique to understand the distribution, classification and diversity of GM in specific diseases [68–70]. However, the existing difficulty is that current 16S rRNA sequencing technique is still not able to distinguish whether the microbiomes are active or not, and there is still a lack of resolution beyond the genus level [71,72]. Nevertheless, with the evolution of sequencing techniques and the improvement of data processing, the above drawbacks may be effectively solved in the near future. In addition, subsequent researches can also further analyze the complex interaction between GM and bone and verify the role of specific strains and metabolites by combining the emerging multi-omics research methods in recent years.

5. Conclusions

To sum up, our data revealed the involvement of GM-bone axis in PMOP and the role of FMT in reshaping the status of GM and ameliorating the bone loss in mice with OVX-induced OP. Estrogen-deficiency disrupted the intestinal mucosal barrier, and the interaction between the GM, SCFAs and host inflammatory system altered accordingly. On this basis, FMT inhibited the excessive osteoclastogenesis and prevented the bone loss by correcting imbalance of GM, improving fecal SCFAs level, optimizing intestinal permeability and suppressing release of pro-osteoclastogenic cytokines. FMT treatment might be an alternative option to serve as a promising candidate for the prevention and treatment of PMOP in the future, although these findings still need to be further verified by further animal experiments and human prospective trials with larger sample sizes.

Authorship contribution statement

Yuan-Wei Zhang: Methodology, Validation, Formal analysis, Data curation, Writing – original draft, Writing – review & editing, Visualization. Mu-Min Cao: Methodology, Data curation, Writing – review & editing, Visualization, Project administration. Ying-Juan Li: Investigation, Data curation, Formal analysis, Writing – review & editing. Pan–Pan Lu: Methodology, Project administration, Formal analysis, Data curation, Writing – review & editing. Guang-Chun Dai: Methodology, Project administration, Writing – review & editing. Ming Zhang: Methodology, Data curation, Writing – review & editing. Hao Wang: Methodology, Data curation, Writing – review & editing. Yun-Feng Rui: Methodology, Validation, Project administration, Formal analysis, Writing – original draft, Writing – review & editing, Visualization. All authors approved the final version of manuscript.

Ethical statement

Overall animal experimental designs and schemes were approved by Institutional Animal Care and Use Committee (IACUC) in the School of Medicine, Southeast University (No. 20210510012).

Declaration of competing interest

The authors have no financial or potential competing interests or affiliations with any institution, organization, or company relating to this current manuscript.

Acknowledgements

This current work was supported by grants from Winfast Charity Foundation Project (YL20220525); Jiangsu Provincial Medical Talent, The Project of Invigorating Health Care through Science, Technology and Education (ZDRCA2016083); and Jiangsu Elderly Health Research Project, Key Project of Elderly Health Research Project (LKZ2022010).

Appendix A. Supplementary data

Supplementary data to this article can be found online at https://doi.org/10.1016/j.jot.2022.08.003.

References

[1] Zhu Y, Huang Z, Wang Y, Xu W, Chen H, Xu J, et al. The efficacy and safety of denosumab in postmenopausal women with osteoporosis previously treated with bisphosphonates: a review. J Orthop Translat 2020;22:7–13.
[2] Zhang YW, Lu PP, Li YJ, Dai GC, Cao MM, Xie T, et al. Low dietary choline intake is associated with the risk of osteoporosis in elderly individuals: a population-based study. Food Funct 2021;12(14):6442–51.
[3] Ding M, Overgaard S. 3-D microarchitectural properties and rod- and plate-like trabecular morphometric properties of femur head cancellous bones in patients with rheumatoid arthritis, osteoarthritis, and osteoporosis. J Orthop Translat 2021;28:159–68.
[4] Zhang YW, Cao MM, Li YJ, Dai GC, Lu PP, Zhang M, et al. Dietary protein intake in relation to the risk of osteoporosis in middle-aged and older individuals: a cross-sectional study. J Nutr Health Aging 2022;26(3):252–8.
[5] Xu XM, Li N, Li K, Li XY, Zhang P, Xuan YJ, et al. Discordance in diagnosis of osteoporosis by quantitative computed tomography and dual-energy X-ray absorptiometry in Chinese elderly men. J Orthop Translat 2019;18:59–64.
[6] Melville KM, Kelly NH, Khan SA, Schimenti JC, Ross FP, Main RP, et al. Female mice lacking estrogen receptor-alpha in osteoblasts have compromised bone mass and strength. J Bone Miner Res 2014;29(2):370–9.
[7] Dören M, Samsioe G. Prevention of postmenopausal osteoporosis with oestrogen replacement therapy and associated compounds: update on clinical trials since 1995. Hum Reprod Update 2000;6(5):419–26.
[8] Xing L, Schwarz EM, Boyce BF. Osteoclast precursors, RANKL/RANK, and immunology. Immunol Rev 2005;208:19–29.
[9] Zupan J, Komadina R, Marc J. The relationship between osteoclastogenic and anti-osteoclastogenic pro-inflammatory cytokines differs in human osteoporotic and osteoarthritic bone tissues. J Biomed Sci 2012;19(1):28.
[10] Li J, Geng J, Lin T, Cai M, Sun Y. A mouse model of disuse osteoporosis based on a movable noninvasive 3D-printed unloading device. J Orthop Translat 2022;33:1–12.
[11] Li Y, Pan Q, Xu J, He X, Li HA, Oldridge DA, et al. Overview of methods for enhancing bone regeneration in distraction osteogenesis: potential roles of biometals. J Orthop Translat 2021;27:110–8.
[12] Liu ZJ, Zhang C, Ma C, Qi H, Yang ZH, Wu HY, et al. Automatic phantom-less QCT system with high precision of BMD measurement for osteoporosis screening: technique optimisation and clinical validation. J Orthop Translat 2022;33:24–30.
[13] Qin L, He T, Yang D, Wang Y, Li Z, Yan Q, et al. Osteocyte β1 integrin loss causes low bone mass and impairs bone mechanotransduction in mice. J Orthop Translat 2022;34:60–72.
[14] Tu MY, Han KY, Chang GR, Lai GD, Chang KY, Chen CF, et al. Kefir peptides prevent estrogen deficiency-induced bone loss and modulate the structure of the gut microbiota in ovariectomized mice. Nutrients 2020;12(11):3432.
[15] Chen X, Zhang Z, Hu Y, Cui J, Zhi X, Li X, et al. Lactulose suppresses osteoclastogenesis and ameliorates estrogen deficiency-induced bone loss in mice. Aging Dis 2020;11(3):629–41.
[16] Zhang YW, Lu PP, Li YJ, Dai GC, Chen MH, Zhao YK, et al. Prevalence, characteristics, and associated risk factors of the elderly with hip fractures: a cross-sectional analysis of nhanes 2005-2010. Clin Interv Aging 2021;16:177–85.
[17] Sjögren K, Engdahl C, Henning P, Lerner UH, Tremaroli V, Lagerquist MK, et al. The gut microbiota regulates bone mass in mice. J Bone Miner Res 2012;27(6):1357–67.
[18] Zhang YW, Li YJ, Lu PP, Dai GC, Chen XX, Rui YF. The modulatory effect and implication of gut microbiota on osteoporosis: from the perspective of "brain-gut-bone" axis. Food Funct 2021;12(13):5703–18.
[19] Zhang YW, Cao MM, Li YJ, Dai GC, Lu PP, Zhang M, et al. The regulative effect and repercussion of probiotics and prebiotics on osteoporosis: involvement of brain-gut-bone axis. Crit Rev Food Sci Nutr 2022:1–19 (Online ahead of print).
[20] Jing Y, Yu Y, Bai F, Wang L, Yang D, Zhang C, et al. Effect of fecal microbiota transplantation on neurological restoration in a spinal cord injury mouse model: involvement of brain-gut axis. Microbiome 2021;9(1):59.
[21] Sun MF, Zhu YL, Zhou ZL, Jia XB, Xu YD, Yang Q, et al. Neuroprotective effects of fecal microbiota transplantation on MPTP-induced Parkinson's disease mice: gut microbiota, glial reaction and TLR4/TNF-α signaling pathway. Brain Behav Immun 2018;70:48–60.
[22] Weingarden AR, Vaughn BP. Intestinal microbiota, fecal microbiota transplantation, and inflammatory bowel disease. Gut Microb 2017;8(3):238–52.
[23] Ooijevaar RE, Terveer EM, Verspaget HW, Kuijper EJ, Keller JJ. Clinical application and potential of fecal microbiota transplantation. Annu Rev Med 2019;70:335–51.
[24] Paramsothy S, Nielsen S, Kamm MA, Deshpande NP, Faith JJ, Clemente JC, et al. Specific bacteria and metabolites associated with response to fecal microbiota transplantation in patients with ulcerative colitis. Gastroenterology 2019;156(5).1440-54.e2.
[25] Halkjær SI, Christensen AH, Lo BZS, Browne PD, Günther S, Hansen LH, et al. Faecal microbiota transplantation alters gut microbiota in patients with irritable bowel syndrome: results from a randomised, double-blind placebo-controlled study. Gut 2018;67(12):2107–15.
[26] de Groot P, Nikolic T, Pellegrini S, Sordi V, Imangaliyev S, Rampanelli E, et al. Faecal microbiota transplantation halts progression of human new-onset type 1 diabetes in a randomised controlled trial. Gut 2021;70(1):92–105.
[27] Wang Y, Wiesnoski DH, Helmink BA, Gopalakrishnan V, Choi K, DuPont HL, et al. Fecal microbiota transplantation for refractory immune checkpoint inhibitor-associated colitis. Nat Med 2018;24(12):1804–8.
[28] Yu EW, Gao L, Stastka P, Cheney MC, Mahabamunuge J, Torres Soto M, et al. Fecal microbiota transplantation for the improvement of metabolism in obesity: the FMT-TRIM double-blind placebo-controlled pilot trial. PLoS Med 2020;17(3):e1003051.
[29] Shapiro JM, de Zoete MR, Palm NW, Laenen Y, Bright R, Mallette M, et al. Immunoglobulin A targets a unique subset of the microbiota in inflammatory bowel disease. Cell Host Microbe 2021;29(1):83–93. e3.
[30] Benech N, Legendre P, Radoszycki L, Varriale P, Sokol H. Patient knowledge of gut microbiota and acceptability of fecal microbiota transplantation in various diseases. Neuro Gastroenterol Motil 2022:e14320.
[31] Wang H, Lu Y, Yan Y, Tian S, Zheng D, Leng D, et al. Promising treatment for type 2 diabetes: fecal microbiota transplantation reverses insulin resistance and impaired islets. Front Cell Infect Microbiol 2019;9:455.
[32] Sun K, Zhu J, Deng Y, Xu X, Kong F, Sun X, et al. Gamabufotalin inhibits osteoclastgenesis and counteracts estrogen-deficient bone loss in mice by suppressing RANKL-induced NF-κB and ERK/MAPK pathways. Front Pharmacol 2021;12:629968.
[33] Wen K, Tao L, Tao Z, Meng Y, Zhou S, Chen J, et al. Fecal and serum metabolomic signatures and microbial community profiling of postmenopausal osteoporosis mice model. Front Cell Infect Microbiol 2020;10:535310.
[34] Li B, Liu M, Wang Y, Gong S, Yao W, Li W, et al. Puerarin improves the bone micro-environment to inhibit OVX-induced osteoporosis via modulating SCFAs released by the gut microbiota and repairing intestinal mucosal integrity. Biomed Pharmacother 2020;132:110923.
[35] Schuijt TJ, Lankelma JM, Scicluna BP, de Sousa e Melo F, Roelofs JJ, de Boer JD, et al. The gut microbiota plays a protective role in the host defence against pneumococcal pneumonia. Gut 2016;65(4):575–83.
[36] Caporaso JG, Kuczynski J, Stombaugh J, Bittinger K, Bushman FD, Costello EK, et al. QIIME allows analysis of high-throughput community sequencing data. Nat Methods 2010;7(5):335–6.
[37] Edgar RC. UPARSE: highly accurate OTU sequences from microbial amplicon reads. Nat Methods 2013;10(10):996–8.
[38] Zhu Z, Zhu B, Sun Y, Ai C, Wang L, Wen C, et al. Sulfated polysaccharide from sea cucumber and its depolymerized derivative prevent obesity in association with modification of gut microbiota in high-fat diet-fed mice. Mol Nutr Food Res 2018;62(23):e1800446.
[39] Chen D, Chen G, Wan P, Hu B, Chen L, Ou S, et al. Digestion under saliva, simulated gastric and small intestinal conditions and fermentation in vitro of polysaccharides from the flowers of Camellia sinensis induced by human gut microbiota. Food Funct 2017;8(12):4619–29.
[40] Reid IR. A broader strategy for osteoporosis interventions. Nat Rev Endocrinol 2020;16(6):333–9.
[41] Andreopoulou P, Bockman RS. Management of postmenopausal osteoporosis. Annu Rev Med 2015;66:329–42.
[42] Lan H, Liu WH, Zheng H, Feng H, Zhao W, Hung WL, et al. Bifidobacterium lactis BL-99 protects mice with osteoporosis caused by colitis via gut inflammation and gut microbiota regulation. Food Funct 2022;13(3):1482–94.
[43] Schepper JD, Collins F, Rios-Arce ND, Kang HJ, Schaefer L, Gardinier JD, et al. Involvement of the gut microbiota and barrier function in glucocorticoid-induced osteoporosis. J Bone Miner Res 2020;35(4):801–20.
[44] Ma S, Wang N, Zhang P, Wu W, Fu L. Fecal microbiota transplantation mitigates bone loss by improving gut microbiome composition and gut barrier function in aged rats. PeerJ 2021;9:e12293.
[45] Wang N, Ma S, Fu L. Gut microbiota dysbiosis as one cause of osteoporosis by impairing intestinal barrier function. Calcif Tissue Int 2022;110(2):225–35.
[46] Fuhrman BJ, Feigelson HS, Flores R, Gail MH, Xu X, Ravel J, et al. Associations of the fecal microbiome with urinary estrogens and estrogen metabolites in postmenopausal women. J Clin Endocrinol Metab 2014;99(12):4632–40.
[47] Flores R, Shi J, Fuhrman B, Xu X, Veenstra TD, Gail MH, et al. Fecal microbial determinants of fecal and systemic estrogens and estrogen metabolites: a cross-sectional study. J Transl Med 2012;10:253.
[48] Adeel S, Singh K, Vydareny KH, Kumari M, Shah E, Weitzmann MN, et al. Bone loss in surgically ovariectomized premenopausal women is associated with T lymphocyte activation and thymic hypertrophy. J Invest Med 2013;61(8):1178–83.
[49] D'Amelio P, Grimaldi A, Di Bella S, Brianza SZM, Cristofaro MA, Tamone C, et al. Estrogen deficiency increases osteoclastogenesis up-regulating T cells activity: a key mechanism in osteoporosis. Bone 2008;43(1):92–100.
[50] Macdonald TT, Monteleone G. Immunity, inflammation, and allergy in the gut. Science 2005;307(5717):1920–5.
[51] Turner JR. Intestinal mucosal barrier function in health and disease. Nat Rev Immunol 2009;9(11):799–809.

[52] van den Heuvel EG, Schoterman MH, Muijs T. Transgalactooligosaccharides stimulate calcium absorption in postmenopausal women. J Nutr 2000;130(12):2938–42.
[53] Collins FL, Irwin R, Bierhalter H, Schepper J, Britton RA, Parameswaran N, et al. Lactobacillus reuteri 6475 increases bone density in intact females only under an inflammatory setting. PLoS One 2016;11(4):e0153180.
[54] Clemente JC, Manasson J, Scher JU. The role of the gut microbiome in systemic inflammatory disease. BMJ 2018;360:j5145.
[55] Wang Z, Chen K, Wu C, Chen J, Pan H, Liu Y, et al. An emerging role of Prevotella histicola on estrogen deficiency-induced bone loss through the gut microbiota-bone axis in postmenopausal women and in ovariectomized mice. Am J Clin Nutr 2021;114(4):1304–13.
[56] Vieira AT, Castelo PM, Ribeiro DA, Ferreira CM. Influence of oral and gut microbiota in the health of menopausal women. Front Microbiol 2017;8:1884.
[57] Pacifici R. Bone remodeling and the microbiome. Cold Spring Harb Perspect Med 2018;8(4).
[58] Liu H, Xu Y, Cui Q, Liu N, Chu F, Cong B, et al. Effect of psoralen on the intestinal barrier and alveolar bone loss in rats with chronic periodontitis. Inflammation 2021;44(5):1843–55.
[59] Luu M, Riester Z, Baldrich A, Reichardt N, Yuille S, Busetti A, et al. Microbial short-chain fatty acids modulate CD8(+) T cell responses and improve adoptive immunotherapy for cancer. Nat Commun 2021;12(1):4077.
[60] Carley AN, Maurya SK, Fasano M, Wang Y, Selzman CH, Drakos SG, et al. Short-chain fatty acids outpace ketone oxidation in the failing heart. Circulation 2021;143(18):1797–808.
[61] Weaver CM. Diet, gut microbiome, and bone health. Curr Osteoporos Rep 2015;13(2):125–30.
[62] Kim DE, Kim JK, Han SK, Jang SE, Han MJ, Kim DH. Lactobacillus plantarum NK3 and bifidobacterium longum NK49 alleviate bacterial vaginosis and osteoporosis in mice by suppressing NF-κB-Linked TNF-α expression. J Med Food 2019;22(10):1022–31.
[63] Yan J, Herzog JW, Tsang K, Brennan CA, Bower MA, Garrett WS, et al. Gut microbiota induce IGF-1 and promote bone formation and growth. Proc Natl Acad Sci U S A 2016;113(47). E7554-e63.
[64] Zhou HY, Guo B, Lufumpa E, Li XM, Chen LH, Meng X, et al. Comparative of the effectiveness and safety of biological agents, tofacitinib, and fecal microbiota transplantation in ulcerative colitis: systematic review and network meta-analysis. Immunol Invest 2021;50(4):323–37.
[65] Green JE, Davis JA, Berk M, Hair C, Loughman A, Castle D, et al. Efficacy and safety of fecal microbiota transplantation for the treatment of diseases other than Clostridium difficile infection: a systematic review and meta-analysis. Gut Microb 2020;12(1):1–25.
[66] Gheorghe CE, Ritz NL, Martin JA, Wardill HR, Cryan JF, Clarke G. Investigating causality with fecal microbiota transplantation in rodents: applications, recommendations and pitfalls. Gut Microb 2021;13(1):1941711.
[67] Zhang T, Lu G, Zhao Z, Liu Y, Shen Q, Li P, et al. Washed microbiota transplantation vs. manual fecal microbiota transplantation: clinical findings, animal studies and in vitro screening. Protein Cell 2020;11(4):251–66.
[68] Whelan FJ, Surette MG. A comprehensive evaluation of the sl1p pipeline for 16S rRNA gene sequencing analysis. Microbiome 2017;5(1):100.
[69] Shahi SK, Zarei K, Guseva NV, Mangalam AK. Microbiota analysis using two-step PCR and next-generation 16S rRNA gene sequencing. JoVE 2019;(152).
[70] Abellan-Schneyder I, Matchado MS, Reitmeier S, Sommer A, Sewald Z, Baumbach J, et al. Primer, pipelines, parameters: issues in 16S rRNA gene sequencing. mSphere 2021;6(1).
[71] Zou Y, Xue W, Luo G, Deng Z, Qin P, Guo R, et al. 1,520 reference genomes from cultivated human gut bacteria enable functional microbiome analyses. Nat Biotechnol 2019;37(2):179–85.
[72] Piquer-Esteban S, Ruiz-Ruiz S, Arnau V, Diaz W, Moya A. Exploring the universal healthy human gut microbiota around the World. Comput Struct Biotechnol J 2022;20:421–33.